Contribution from the Department of Chemistry and Biochemistry, University of California, Los Angeles, California 90024

Substitution by Trialkyl Phosphites on $[C(NMe_2)_3][Ru_3\{\mu\text{-}O{=}C(NMe_2)\}(CO)_{10}]$: Crystal and Molecular Structure of $Ru_3\{\mu\text{-}H,\mu\text{-}O{=}C(NMe_2)\}(CO)_9P(OPh)_3$

ANDREAS MAYR, YING CHIH LIN, NEIL M. BOAG, CARSTEN E. KAMPE, CAROLYN B. KNOBLER, and HERBERT D. KAESZ*

Received July 12, 1984

The salt $[C(NMe_2)_3][Ru_3\{\mu\text{-}O{=}C(NMe_2)\}(CO)_{10}]$ ([Gua][**2a**]) is obtained in essentially 100% spectroscopic yield from the reaction of $Ru_3(CO)_{12}$ with $C(NMe_2)_4$. In tetrahydrofuran, [Gua][**2a**] undergoes substitution by L to give [Gua]-$[Ru_3\{\mu\text{-}O{=}C(NMe_2)\}(CO)_9L]$, within 10 min for L = $P(OMe)_3$, within 20 min for L = $P(OEt)_3$, or within 3.5 h for L = $P(OPh)_3$. ^{13}C NMR of [Gua][**2a**] indicates stereochemical nonrigidity in THF. A limiting spectrum is obtained at −100 °C indicating the presence of three bridging CO groups. Acidification of the salts with CF_3SO_3H gives the neutral derivatives $Ru_3\{\mu\text{-}H,\mu\text{-}O{=}C(NMe_2)\}(CO)_9P(OR)_3$, R = Me (**3**), Et (**4**), Ph (**5**), in isolated yields of 55, 42, and 45%, respectively. The structure of **5** has been determined at −158 °C with a Syntex P$\bar{1}$ computer-automated diffractometer and graphite-monochromated Mo Kα radiation. The complex crystallizes in the *Pc* space group in a cell having dimensions a = 18.434 (3) Å, b = 10.166 (4) Å, c = 19.741 (7) Å, and β = 114.90 (2)°. The cell volume is 3355 (2) Å^3, and the calculated density is ρ = 3.72 g cm^{-3}. The structure was solved by a combination of Patterson and Fourier techniques and refined by full-matrix least squares to give a final R_F = 0.030 and R_{wF} = 0.037. There are two crystallographically distinct molecules in the unit cell: Ru(1–3), molecule 1; Ru(4–6), molecule 2. The three ruthenium atoms of each molecule define a triangle of unequal sides (± 0.002 Å): Ru(1)–Ru(2) = Ru(4)–Ru(5) = 2.884, Ru(1)–Ru(3) = 2.830, Ru(4)–Ru(6) = 2.841, and Ru(2)–Ru(3) = Ru(5)–Ru(6) = 2.856. Both the hydrogen atom and the carboxamido group bridge Ru(1)–Ru(2) on opposite sides of the trimetal plane. The carboxamido group is coordinated through the carbon and oxygen atoms. The $P(OPh)_3$ group is attached to the Ru atom to which is bonded the oxygen of the carboxamido group in a position trans to the $Ru(CO)_4$ unit. Partial double-bond character between C and O and between C and N atoms of the carboxamido group is indicated (for molecule 1 and molecule 2, respectively, in Å): C–O, 1.255 (17) and 1.291 (16); C–N, 1.355 (17) and 1.339 (17).

Introduction

Studies of the stepwise substitution of nucleophiles on $Ru_3(CO)_{12}$ (**1**) had led us to prepare the guanidinium salt $[C(NMe_2)_3][Ru_3\{\mu\text{-}O{=}C(NMe_2)\}(CO)_{10}]$ ([Gua][**2a**]) in the reaction of **1** with $C(NMe_2)_4$.[1] ^{13}C NMR studies indicated an isomer for the anion containing three bridging CO groups of the type seen previously only for the neutral (1,2-diazene) complexes $M_3\{\mu\text{-}C_4H_4N_2\}\{\mu\text{-}CO\}_3(CO)_7$, M = Ru,[2a] M = Os.[2b] The salt [Gua][**2a**], however, could not be obtained as a single crystal, and we were therefore prompted to carry out substitution reactions with phosphite ligands hoping to produce a suitable derivative. Substituted salts for $P(OR)_3$, R = Me, Et, Ph ([Gua][**3a**], [Gua][**4a**], [Gua][**5a**], respectively), proved also to be unsuitable for X-ray studies. Since that time, Darensbourg and co-workers have reported the structure of $[N(PPh_3)_2][Ru_3\{\mu\text{-}O{=}C(H)O\}\{\mu\text{-}CO\}_3(CO)_7]$,[3] which provides an example of this isomeric form in an anionic complex.

Acidifying the salts [Gua][**3a**, **4a**, and **5a**] leads to the neutral complexes $Ru_3\{\mu\text{-}H,\mu\text{-}O{=}C(NMe_2)\}(CO)_9P(OR)_3$, R = Me (**3**), Et (**4**) and Ph (**5**), whose structures no longer contain bridging CO groups (^{13}C NMR). Suitable single crystals of the $P(OPh)_3$ complex were obtained, and an X-ray structure was determined unequivocally to establish the position of substitution. The present paper describes these studies. A companion work describes substitution reactions of a series of related edge-double-bridged complexes.[4]

Results and Discussion

Syntheses. The syntheses accomplished in this study are summarized in Scheme I. The intermediate anions and the neutral products after acidification are characterized by IR and NMR, whose data are presented in Tables I and II.

Scheme I

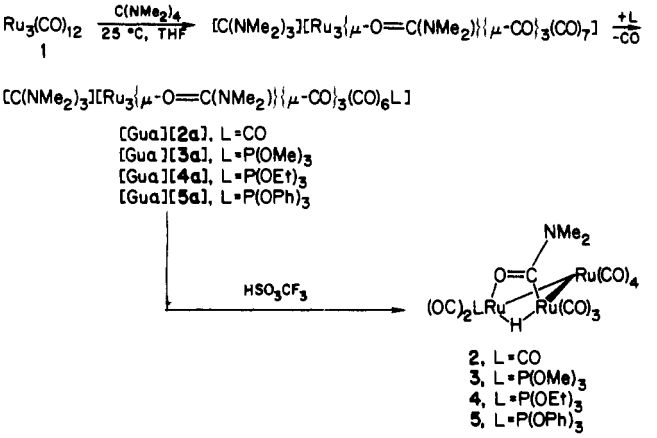

IR Absorptions, 2250–1500 cm^{-1}. Representative traces of the carbonyl absorptions of [Gua][**2a**] and **2** are deposited as supplementary material. The absorptions attributable to terminal carbonyl groups in the anions are broadened and shifted to lower energy as compared to those of the corresponding neutral species (see Table I). The substituted anions consist of a mixture of isomers (see discussion below); their IR bands thus envelop absorptions of several species.

In the bridging carbonyl region, 1815–1775 cm^{-1}, the anions each display a broad band, accompanied by a discernible shoulder on the high-energy side in the spectrum of [Gua][**2a**]. In [**2a**$^-$] three separate environments should be discerned for the bridging CO groups (see structural drawing in Scheme I). These are seen in the ^{13}C NMR (see below). Two of the bridging CO groups, however, are more subtly differentiated than the CO that bridges the same edge as the μ-O=CNMe$_2$ group. With one maximum and one shoulder in the bridging carbonyl region of [**2a**$^-$], the IR proves to be less sensitive for

(1) Mayr, A.; Lin, Y. C.; Boag, N. M.; Kaesz, H. D. *Inorg. Chem.* **1982**, *21*, 1704.
(2) (a) Cotton, F. A.; Hanson, B. E.; Jamerson, J. D. *J. Am. Chem. Soc.* **1977**, *99*, 6588–6594. (b) Cotton, F. A.; Hanson, B. E. *Inorg. Chem.* **1977**, *16*, 2820–2822.
(3) Darensbourg, D. J.; Pala, M.; Walla, J. *Organometallics* **1983**, *2*, 1285–1291.
(4) Kampe, C. E.; Kaesz, H. D. *Inorg. Chem.*, following paper in this issue.

0020-1669/84/1323-4640$01.50/0

Table I. IR Data in the Region 2250–1500 cm^{-1}

compd	ν(CO), cm^{-1}									
[Gua][**2a**][a]	2060 w	2008 s	1986 s	1974 s	1946 sh	1932 m	1813 sh	1796 m		
[Gua][**3a**][a]	2044 w	1988 vs	1959 s	1925 sh	1914 m		1778 br			
[Gua][**4a**][a]	2043 w	1985 vs	1956 s	1925 sh	1912 m		1777 br			
[Gua][**5a**][a]	2047 w	1991 vs	1964 s	1947 m	1931 m		1795 br			
2[b]	2102 m	2065 vs	2051 vs	2024 m	2015 vs	2000 sh	1999 s	1989 vw	1982 w	1957 vw
3	2086 m	2044 vs	2024 m	2019 sh	2011 m	2001 s	1991 w	1985 w	1971 w	
4	2085 m	2043 vs	2023 m	2017 w	2010 w	2000 s	1990 w	1984 w	1971 w	
5	2088 m	2047 vs	2027 m	2014 m		2006 s	1993 m	1989 sh	1972 w	

[a] $[C(NMe_2)_3^+]$: 1601 m, 1577 w cm^{-1}. [b] Cf. ref 5; calibrated FTIR data cited here.

Table II. NMR Data[a,b]

compd	$\delta(^1H)$[c]
2	2.52, 2.31 ($N(CH_3)_2$), −13.78 (s, RuHRu)
3	3.70 (d, $POCH_3$, J_{PH} = 11.24), 3.18, 2.81 ($N(CH_3)_2$), −13.82 (d, RuHRu, J_{PH} = 9.64)
4	4.04 (q, CH_2, J = 7.2), 3.18, 2.80 ($N(CH_3)_2$), 1.32 (t, CH_3, J_{HH} = 7.2), −13.8 (d, RuHRu, J_{PH} = 9.64)
5	7.4–7.1 (m, C_6H_5), 3.10, 2.56 ($N(CH_3)_2$), −14.0 (d, RuHRu), J_{PH} = 11.24)
[Gua][**2a**]	2.99 ($[C(NMe_2)_3^+]$), 2.98, 2.31 ($N(CH_3)_2$)

compd	$\delta(^{13}C)$[c]
5[d]	208.1, 207.1, 204.5 (O=*C*(NMe_2)), 203.2 (J_{PC} = 8.55), 201.4, 197.2 (J_{CH} = 12.2), 196.0 (J_{CH} = 14.6, J_{PC} = 7.32), 194.0, 193.0 (J_{PC} = 22.0), 191.2
[Gua][**2a**][e]	263.3, 257.6, 245.7, 210.5 (O=*C*(NMe_2), 208.9, 205.7, 204.3, 202.7

[a] Solvent $CDCl_3$; coupling constants in Hz. [b] ^{31}P NMR (ppm, relative to 85% H_3PO_4): **3**, 138.30; **4**, 132.34; **5**, 124.69. [c] Relative to Me_4Si; singlets unless otherwise noted. Legend: d = doublet, m = multiplet, t = triplet, q = quintet. [d] For comparison, data for **2** (from ref 5a or 5b, ppm): 206.6, 205.1, 203.3 (O=*C*(NMe_2), 200.5 (2), 195.9 (J_{CH} = 6.3), 194.3 (J_{CH} = 8.4), 192.0 (2), 189.7, 184.3. [e] Limiting spectrum at −100 °C in THF.

making the subtle distinctions. The absorptions of the bridging carboxamido group are to be found in the region 1500–1100 cm^{-1}.[5a] These were not examined in the present series of compounds.

^1H and ^{31}P NMR. In the data of Table II, the features of interest are the μ-^1H–Ru–^{31}P coupling constants, which are consistent with cis relationships between these two nuclei (see companion work for discussion of this point).[4] Spectra of the anions indicate these to be a mixture of isomers. Protonation, however, leads to only one isolable neutral product, perhaps that determined thermodynamically.

^{13}C NMR data were obtained for [Gua][**2a**] (Table II). The resonances of the carbonyl groups (202.7–263.3 ppm) at five different temperatures are shown in Figure 1. The limiting spectrum at −100 °C shows broadening of all resonances due to solvent viscosity. Three distinct resonances are seen near 250 ppm (bridging carbonyl region). The resonances of the seven terminal carbonyl groups and that of the carboxamido carbon (O=*C*NMe_2) are seen closely spaced around 200 ppm. The resonance of the carboxamido carbon and that of the carbon atom in the cation are unaffected as the temperature is raised. The former resonance is identified by its appearance as a sharp singlet throughout the range where the other resonances in the carbonyl region undergo various changes.

At −60 °C only three sharp resonances are seen accompanied by a broad peak centered at 227.7 ppm. Observation of

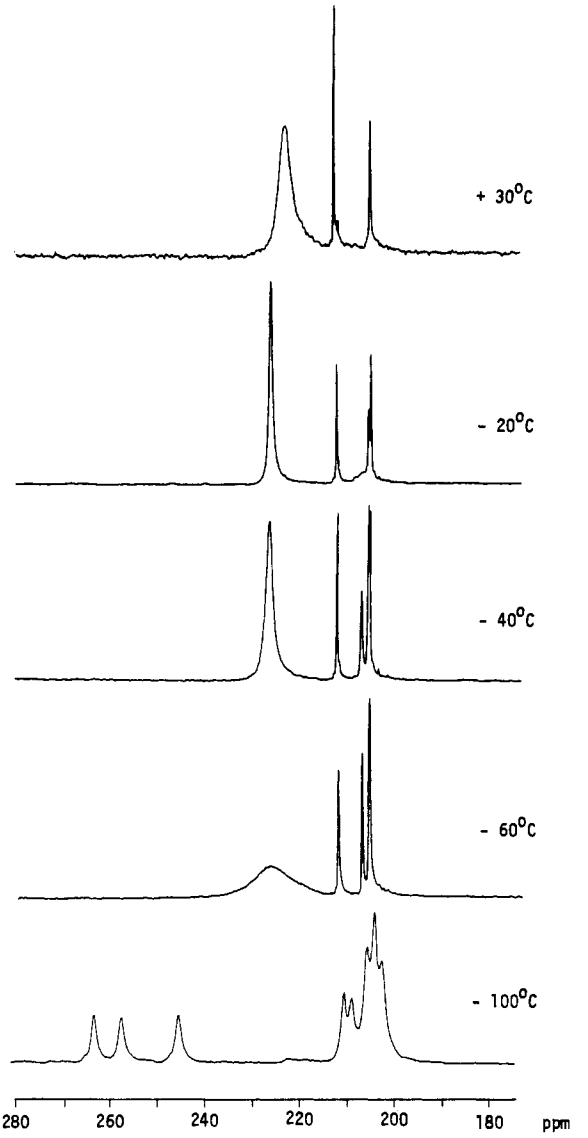

Figure 1. Variable-temperature $^{13}C\{^1H\}$ NMR spectra in the carbonyl region of ^{13}CO-enriched $[C(NMe_2)_3][Ru_3(\mu\text{-}O{=}CNMe_2)(CO)_{10}]$ ([Gua][**2a**]) (chemical shifts relative to Me_4Si, solvent THF-d_8, $Cr(acac)_3$ (0.05 M) added as a paramagnetic relaxation agent).

an "in-plane" exchange in other complexes[6] prompts us to suggest a similar exchange between the three bridging carbonyl groups and the three carbonyl groups terminally bonded in a *radial* position (one on each of the three metal atoms). The area under the three sharp resonances represents only three carbonyl groups and the carboxamido carbon. Thus, the exchange process at this temperature must also involve one of

(5) (a) Szostak, R. Dissertation, University of California, Los Angeles, CA, 1980. (b) Szostak, R.; Strouse, C. E.; Kaesz, H. D. *J. Organomet. Chem.* **1980**, *191*, 243–260.

(6) Johnson, B. F. G.; Benfield, R. E. In "Transition Metal Clusters"; Johnson, B. F. G., Ed.; Wiley-Interscience: New York, 1980; Chapter VII.

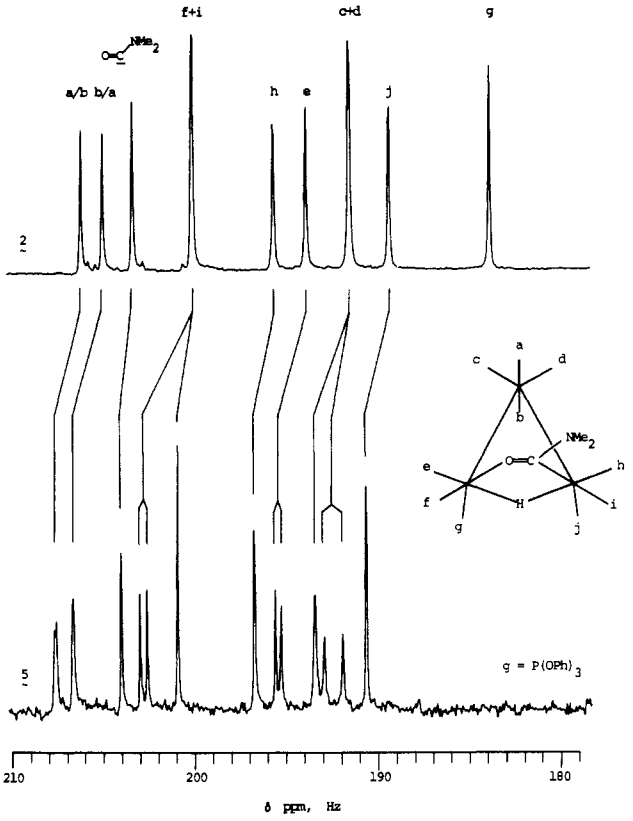

Figure 2. $^{13}C\{^1H\}$ NMR spectra in the carbonyl region ($CDCl_3$ solution with $Cr(acac)_3$ (0.05 M), 25 °C): (upper trace) $Ru_3\{\mu\text{-}H,\mu\text{-}O{=}CNMe_2\}(CO)_{10}$ (**2**);[5a] (lower trace) $Ru_3\{\mu\text{-}H,\mu\text{-}O{=}CNMe_2\}(CO)_9P(OPh)_3$ (**5**).

the axially bonded terminal carbonyl groups.

Increase in temperature to −40 °C reveals a doublet nature of the high-field signal, suggesting assignment of these peaks to two *axial* carbonyl groups and the accompanying peak at 208.9 ppm to a third such group. Further increase in temperature brings about the collapse of two of the remaining sharp carbonyl peaks, leaving at 30 °C only a single sharp resonance (in addition of course to the carboxamido group resonance) representing a unique *axial* carbonyl group not participating in exchange with the other groups. This too begins to broaden at 50 °C (not shown in Figure 1). As an assignment for this peak we suggest the carbonyl group axially coordinated in a position trans to the carbon of the carboxamido group.

The ^{13}C NMR spectrum of **5** is shown in Figure 2 and related to that of **2**.[5] The data for these two spectra are given in Table II. Assignment of these peaks comes from the pattern of $^{31}P\text{–}^{13}C(O)$ coupling shown in Figure 2 as well as $^1H\text{–}^{13}C(O)$ coupling (not shown here). The assignments parallel those presented for like-substituted derivatives, for reasons discussed in detail in the companion paper.[4]

Experimental Section

Synthesis of $Ru_3\{\mu\text{-}H,\mu\text{-}O{=}C(NMe_2)\}(CO)_9P(OR)_3$: R = Me (3), Et (4), Ph (5). The same synthetic procedure, with small variations as explained below, may be used for all three derivatives; yields reported below are based on $Ru_3(CO)_{12}$ (**1**). To a solution of **1** (100 mg, 0.16 mmol) in 75 mL of THF is added $C(NMe_2)_4$ (30 mg, 0.16 mmol). The solution is stirred for 1 h at 25 °C to permit formation of $[Gua][Ru_3\{\mu\text{-}O{=}C(NMe_2)\}(CO)_{10}]$ ([Gua][**2a**]). At this point phosphite is added and the solution stirred to permit substitution. For $P(OMe)_3$, 20 mg (0.16 mmol) is added and 10 min is required for complete substitution (determined by the disappearance of the characteristic infrared stretching frequencies of **2** in the metal carbonyl region). For the same molar quantity of $P(OEt)_3$, 20 min is required. For $P(OPh)_3$, 0.19 mmol is added and 3.5 h is required. Next, 0.16 mmol of CF_3SO_3H is added (0.1 M solution in diethyl ether), the solvents are removed under vacuum, and the residue is redissolved in 5 mL of CH_2Cl_2 to which 20 mL of hexane is added. The solvent volume is brought down to 10 mL under reduced pressure. Solids are allowed to settle, and the supernatant liquid is decanted. This process is repeated once more. The combined extracts are reduced in volume under vacuum and redissolved in hexane. The product is purified by chromatography on silica gel, by eluting first with hexane and then with increasing concentrations of CH_2Cl_2. **3**, a brown-orange, crystalline material, elutes with 3:1 hexane/CH_2Cl_2; yield 66 mg (0.088 mmol, 55%). **4**, also a brown-orange crystalline material, elutes with 3:1 hexane/CH_2Cl_2; yield 52 mg (0.066 mmol, 42%). **5**, an orange crystalline material, is eluted first with 4:1 hexane/CH_2Cl_2 and then rechromatographed eluting with a 9:1 ratio of that solvent mix; yield 68 mg (0.072 mmol, 45%). Anal. Calcd for $Ru_3\{\mu\text{-}H,\mu\text{-}O{=}C(NMe_2)\}(CO)_9P(OPh)_3$ (**5**), $C_{30}H_{22}NO_{13}PRu_3$: C, 38.39; H, 2.36; N, 1.49; P, 3.30. Found (Schwartzkopf Microanalytical Laboratory, Woodside, NY 11377): C, 40.01; H, 2.71; N, 1.37; P, 3.60.

Structure Determination of $Ru_3\{\mu\text{-}H,\mu\text{-}O{=}C(NMe_2)\}(CO)_9P(OPh)_3$. Data Collection. Suitable crystals of $Ru_3\{\mu\text{-}H,\mu\text{-}O{=}C(NMe_2)\}(CO)_9P(OPh)_3$ were grown from hexane solution at −20 °C. Preliminary photographs indicated a monoclinic system. Weissenberg photographs of (*h*0*l*) and (*h*1*l*) showed systematic absences for reflections (*h*0*l*), *l* = odd. In addition, diffractometer data showed absences for reflections (0*k*0), *k* = odd. Space group $P2_1/c$ with cell parameters of $a = 18.56$ Å, $b = 10.29$ Å, $c = 19.98$ Å, and $\beta = 114.8°$ was assumed. It was later found from the data collection that the space group is *Pc* where the reflections (0*k*0) for $k = 2n + 1$ are coincidentally weak.

The crystal was moved to a Syntex $P\bar{1}$ diffractometer and mounted with the faces (*hk*0), where *h* and *k* = ±1, roughly parallel to the instrumental ϕ axis.

Fifteen strong reflections selected from a Polaroid photograph were used as input to the automatic centering, autoindexing, and least-squares routines of the diffractometer to obtain a set of low-temperature lattice parameters. The refined unit cell parameters and specifics related to data collection are given in Table III.

Intensity data were collected with use of the $\theta/2\theta$ scan technique with Mo Kα radiation, a scan rate of 3.0° min^{-1}, and a scan range

Table III. Crystal and Intensity Collection Data for **5**[a,b]

molecule	$Ru_3\{\mu\text{-}H,\mu\text{-}O{=}C(NMe_2)\}(CO)_9P(OPh)_3$
fw	938
a, Å	18.434 (3)
b, Å	10.166 (4)
c, Å	19.741 (7)
β, deg	114.90 (2)
V, Å^3	3355 (2)
Z	8
ρ(calcd), g cm^{-3}	3.72
space group	*Pc*
cryst size, mm	0.01, 0.05, 0.25
boundary faces	100, 110, $\bar{1}00$, $\bar{1}10$, $1\bar{1}0$, $\bar{1}\bar{1}0$, 001, $00\bar{1}$[f]
abs coeff, μ, cm^{-1}	14.17
transmission factors	0.295–0.552
scan rate, deg min^{-1}	3.0
scan range	
below Kα_1, deg	1.5
above Kα_2, deg	1.5
2θ limits, deg	50
observns	$h,k,\pm l$
total measd data	5943
no. of unique data ($I_o > 3\sigma(I_o)$)	4593
total no. of variables	492
R_F[c]	0.030
R_{wF}[d]	0.037
S[e]	1.05

[a] Temperature 115 K. [b] Radiation source: Mo Kα (graphite monochromated), $\lambda = 0.7107$ Å. [c] $R = \Sigma(|F_o| - |F_c|)/\Sigma|F_o|$. [d] $R_w = [\Sigma w(|F_o| - |F_c|)^2/\Sigma w|F_o|^2]^{1/2}$, $w = 1/(\sigma^2|F_o|)$. [e] Error in observation of unit weight. Goodness of fit = $[\Sigma w(|F_o| - |F_c|)^2/(N_o - N_v)]^{1/2}$, where N_o is the number of observations and N_v is the number of variables. [f] At distances (mm) of 0.01, 0.01, 0.0, 0.05, 0.05, 0.0, 0.0, and 0.25, respectively, from a common point.

Table IV. Fractional Atomic Coordinates[a] for Nongroup Atoms of $Ru_3\{\mu$-H,μ-O=C(NMe_2)$\}(CO)_9P(OPh)_3$

atom	x	y	z	atom	x	y	z
			Molecule A				
Ru(1)	0.0000	−0.0001 (1)	0.0000	O(12)	0.0196 (6)	0.2480 (10)	0.0901 (5)
Ru(2)	−0.1075 (1)	−0.1198 (1)	−0.1385 (1)	O(21)	−0.2741 (6)	−0.0636 (12)	−0.2566 (6)
Ru(3)	−0.1674 (1)	0.0228 (1)	−0.0482 (1)	O(22)	−0.1472 (6)	−0.3930 (9)	−0.0946 (7)
P(1)	0.1326 (3)	−0.0238 (4)	0.0299 (2)	O(23)	−0.0364 (6)	−0.2435 (11)	−0.2373 (6)
N(1)	−0.0683 (7)	0.1272 (12)	−0.2142 (7)	O(31)	−0.1491 (6)	−0.2356 (10)	0.0360 (6)
C(1)	−0.0588 (8)	0.0604 (13)	−0.1516 (8)	O(32)	−0.1628 (7)	0.2780 (10)	−0.1314 (7)
C(3)	−0.0272 (10)	0.2502 (15)	−0.2083 (10)	O(33)	−0.3490 (6)	0.0011 (11)	−0.1333 (7)
C(4)	−0.1276 (11)	0.0871 (17)	−0.2909 (10)	O(34)	−0.1543 (6)	0.1663 (9)	0.0910 (6)
C(11)	0.0102 (9)	−0.1041 (16)	0.0831 (10)	O(71)	0.1838 (5)	−0.0070 (8)	0.1186 (5)
C(12)	0.0124 (7)	0.1551 (12)	0.0565 (7)	O(72)	0.1696 (5)	−0.1528 (8)	0.0100 (5)
C(21)	−0.2135 (9)	−0.0835 (15)	−0.2119 (9)	O(73)	0.1754 (4)	0.0827 (8)	−0.0006 (4)
C(22)	−0.1353 (7)	−0.2916 (13)	−0.1092 (7)	H(1)	−0.028 (10)	−0.163 (15)	−0.061 (10)
C(23)	−0.0619 (8)	−0.1996 (13)	−0.2001 (8)	H(3A)	0.02	0.23	−0.20
C(31)	−0.1552 (8)	−0.1436 (14)	0.0044 (8)	H(3B)	−0.04	0.27	−0.26
C(32)	−0.1613 (10)	0.1830 (17)	−0.1009 (10)	H(3C)	−0.05	0.33	−0.20
C(33)	−0.2828 (8)	0.0060 (12)	−0.1036 (7)	H(4A)	−0.15	−0.01	−0.29
C(34)	−0.1624 (8)	0.1143 (13)	0.0357 (7)	H(4B)	−0.10	0.07	−0.32
O(1)	−0.0094 (5)	0.1142 (9)	−0.0931 (5)	H(4C)	−0.16	0.15	−0.31
O(11)	0.0200 (6)	−0.1585 (11)	0.1363 (6)				
			Molecule B				
Ru(4)	0.5280 (1)	0.5092 (1)	−0.0343 (1)	O(41)	0.5148 (6)	0.6604 (11)	−0.1691 (6)
Ru(5)	0.6483 (1)	0.6255 (1)	0.0987 (1)	O(42)	0.4800 (5)	0.2692 (10)	−0.1344 (5)
Ru(6)	0.6927 (1)	0.4665 (1)	0.0030 (1)	O(51)	0.6966 (6)	0.8867 (10)	0.0486 (6)
P(2)	0.3982 (2)	0.5554 (3)	−0.0588 (2)	O(52)	0.8180 (6)	0.5495 (12)	0.2091 (6)
N(2)	0.6081 (7)	0.3984 (10)	0.1833 (6)	O(53)	0.5950 (7)	0.7802 (10)	0.2007 (6)
C(2)	0.5955 (8)	0.4576 (13)	0.1187 (7)	O(61)	0.6870 (6)	0.7189 (9)	−0.0845 (6)
C(5)	0.5647 (9)	0.2772 (14)	0.1823 (8)	O(62)	0.6881 (7)	0.2260 (11)	0.0956 (7)
C(6)	0.6673 (11)	0.4380 (18)	0.2557 (9)	O(63)	0.8766 (6)	0.4685 (11)	0.0756 (7)
C(41)	0.5206 (7)	0.6024 (13)	−0.1165 (7)	O(64)	0.6602 (6)	0.3015 (10)	−0.1358 (6)
C(42)	0.4990 (7)	0.3573 (12)	−0.0951 (7)	O(81)	0.3678 (5)	0.6995 (8)	−0.0494 (4)
C(51)	0.6796 (9)	0.7864 (15)	0.0649 (9)	O(82)	0.3447 (5)	0.5227 (8)	−0.1445 (5)
C(52)	0.7522 (9)	0.5780 (16)	0.1674 (9)	O(83)	0.3499 (4)	0.4725 (8)	−0.0222 (4)
C(53)	0.6126 (8)	0.7232 (13)	0.1615 (8)	H(2)	0.562 (10)	0.626 (15)	0.022 (10)
C(61)	0.6874 (8)	0.6279 (13)	−0.0480 (8)	H(5A)	0.50	0.28	0.15
C(62)	0.6883 (8)	0.3193 (14)	0.0619 (8)	H(5B)	0.56	0.26	0.21
C(63)	0.8096 (8)	0.4670 (12)	0.0489 (7)	H(5C)	0.58	0.20	0.15
C(64)	0.6737 (7)	0.3617 (12)	−0.0832 (7)	H(6A)	0.68	0.52	0.26
O(2)	0.5418 (6)	0.4012 (9)	0.0606 (5)	H(6B)	0.63	0.44	0.28
				H(6C)	0.71	0.37	0.27

[a] Estimated standard deviations in the least significant figure(s) are given in parentheses in this and the subsequent table; atoms are labeled according to Figure 2.

of 1.5° below the Mo $K\alpha_1$ peak to 1.5° above the Mo $K\alpha_2$ peak. Background counts were taken, equal to half the count time of the scan, at each end of the scan range. The intensities of the three standard reflections $(13\bar{4})$, $(\bar{6}0\bar{2})$, and $(\bar{3}0\bar{2})$ were recorded after every 97 intensity measurements throughout the data collection to monitor crystal and diffractometer stability. Variations in the standards were random; all measurements were within a factor of 1.2σ of the respective mean values. A total of 5943 independent reflections were measured, constituting a quarter-sphere $+h,+k,\pm l$ accessible with Mo $K\alpha$ radiation and $0° < 2\theta < 50°$. The 1350 reflections having $I < 3\sigma(I)$ were considered to be unobserved and were omitted from the refinement. The 4593 observed reflections were corrected for Lorentz and polarization effects and converted to $|F_o|$ and $\sigma(|F_o|)$ by means of the DATARED program (see below); absorption corrections were applied.

Solution and Refinement. All calculations were performed on a VAX 11/780 computer. Programs used for the structure determination consist in all cases of local modifications edited by Dr. C. E. Strouse and his research group.[7] Scattering factors for neutral ruthenium, nitrogen, phosphorus, oxygen, and carbon atoms were taken from Table 2.2A of ref 8a while those for hydrogen were from Stewart et al.[8b] Both real ($\Delta f'$) and imaginary ($\Delta f''$) components of anomalous dispersion were included for ruthenium and phosphorus by using the values in Table 2.3.1 of ref 8a.

The solution for the structure of **5** was obtained by a combination of Patterson and difference Fourier analyses. The positions of the six ruthenium atoms, which constitute two symmetry-unrelated trimetal frameworks, were obtained from a three-dimensional Patterson map. Full-matrix least-squares refinement on these atoms with isotropic temperature factors produced the residuals $R_F = 0.133$ and $R_{wF} = 0.189$. A difference Fourier synthesis revealed the positions of all remaining nonhydrogen atoms. The carbon atoms of the phenyl rings of the phosphite ligand were refined as rigid bodies under D_{6h} symmetry with C–C distances of 1.392 Å and individually assigned isotropic temperature factors. Refinement with isotropic temperature factors for all atoms produced the residuals $R_F = 0.066$ and $R_{wF} = 0.080$. The data were then corrected for the effects of absorption (see Table III, applied to F^2). Two cycles of least-squares refinement of positional and isotropic thermal parameters decreased the residuals to $R_F = 0.041$ and $R_{wF} = 0.049$, indicating the validity of the correction. In order to maintain a high ratio of number of data to number of variables, in further cycles of refinement, the following atoms were continued to be refined isotropically: C of the CO groups and of the Me groups in the bridging O=$CNMe_2$ group, and O of the $P(OMe)_3$ groups. Three more cycles of least-squares refinement were carried out with anisotropic thermal parameters assigned to the remaining nongroup,

(7) Functions and programs employed are given as follows: data reduction, DATARED, programs for control of the Syntex diffractometer locally written by C. E. Strouse and co-workers; Patterson and Fourier programs, adapted from algorithms in MULTAN78, P. Main (University of York, England); full-matrix least squares and error analysis, ORFLS and ORFFE, W. R. Busing, K. O. Martin, and H. A. Levy (Oak Ridge National Laboratory); absorption correction, ABSN, P. Coppens; least-squares planes, MGTL, P. Gantzel and K. N. Trueblood; thermal ellipsoid plot program, ORTEP II, C. K. Johnson (Oak Ridge National Laboratory); structure factor table listing, PUBLIST, E. Hoel.

(8) (a) "International Tables for X-ray Crystallography"; Kynoch Press: Birmingham, England, 1975; Vol. IV. (b) Stewart, R. F.; Davidson, E. R.; Simpson, W. T. *J. Chem. Phys.* **1965**, *42*, 3175.

Table V. Bond Lengths (Å) and Bond Angles (deg) in $Ru_3\{\mu\text{-}H,\mu\text{-}O{=}C(NMe_2)\}(CO)_9P(OPh)_3$[a]

molecule A		molecule B	
Ru(1)-Ru(2)	2.884 (2)	Ru(4)-Ru(5)	2.884 (2)
Ru(1)-Ru(3)	2.830 (2)	Ru(4)-Ru(6)	2.841 (2)
Ru(2)-Ru(3)	2.856 (2)	Ru(5)-Ru(6)	2.856 (2)
Ru(1)-O(1)	2.118 (9)	Ru(4)-O(2)	2.092 (9)
Ru(1)-P(1)	2.270 (4)	Ru(4)-P(2)	2.281 (4)
Ru(1)-H(1)	1.98 (16)	Ru(4)-H(2)	1.57 (16)
Ru(2)-C(1)	2.102 (13)	Ru(5)-C(2)	2.084 (13)
Ru(2)-H(1)	1.67 (18)	Ru(5)-H(2)	1.67 (17)
C(1)-O(1)	1.255 (17)	C(2)-O(2)	1.291 (16)
C(1)-N(1)	1.355 (17)	C(2)-N(2)	1.339 (17)
Ru(1)-Ru(3)-Ru(2)	61.007 (43)	Ru(4)-Ru(6)-Ru(5)	60.790 (43)
Ru(3)-Ru(2)-Ru(1)	59.074 (44)	Ru(6)-Ru(5)-Ru(4)	59.350 (43)
Ru(2)-Ru(1)-Ru(3)	59.919 (43)	Ru(5)-Ru(4)-Ru(6)	59.860 (45)
P(1)-Ru(1)-Ru(3)[b]	175.62 (10)	P(2)-Ru(4)-Ru(6)	176.11 (11)
P(1)-Ru(1)-C(11)[c]	90.63 (48)	P(2)-Ru(4)-C(41)	91.47 (39)
P(1)-Ru(1)-C(12)[d]	94.93 (38)	P(2)-Ru(4)-C(42)	92.44 (38)
P(1)-Ru(1)-O(1)[e]	88.31 (26)	P(2)-Ru(4)-O(2)	91.16 (27)
Ru(3)-Ru(1)-C(11)[f]	91.97 (47)	Ru(6)-Ru(4)-C(41)	88.89 (38)
Ru(3)-Ru(1)-C(12)[g]	88.56 (37)	Ru(6)-Ru(4)-C(42)	91.45 (37)
P(1)-Ru(1)-O(1)	88.31 (26)	P(2)-Ru(4)-O(2)	91.16 (27)
O(1)-C(1)-Ru(2)	116.67 (97)	O(2)-C(2)-Ru(5)	116.06 (91)
N(1)-C(1)-Ru(2)	130.5 (10)	N(2)-C(2)-Ru(5)	129.9 (10)
Ru(1)-O(1)-C(1)	108.78 (83)	Ru(4)-O(2)-C(2)	108.78 (80)
O(1)-Ru(1)-H(1)	92 (5)	O(2)-Ru(4)-H(2)	84 (6)
C(1)-Ru(2)-H(1)	95 (5)	C(2)-Ru(5)-H(2)	80 (6)

[a] Related bond lengths and angles in molecules A and B are juxtaposed for ease of comparison. Related angles in **2**[5b] have the values (deg) given in footnotes *b-f*. [b] Ru(3)-Ru(1)-C(12) = 171.9 (2). [c] C(12)-Ru(1)-C(11) = 92.5 (3). [d] C(12)-Ru(1)-C(13) = 98.8 (3). [e] C(12)-Ru(1)-O = 89.7 (3). [f] Ru(3)-Ru(1)-C(11) = 85.9 (2). [g] Ru(3)-Ru(1)-C(13) = 89.1 (3).

nonhydrogen atoms; the discrepancy indices at this point were R_F = 0.031 and R_{wF} = 0.037.

Following this refinement, a difference Fourier map indicated the position of a hydrogen atom bridging ruthenium atoms Ru(2) and Ru(1) and another bridging Ru(5) and Ru(4); their positional parameters were refined with the isotropic thermal parameter arbitrarily assigned as 4.0 Å^2. Positional and thermal parameters of these bridging atoms and the methyl hydrogen atoms were not included in the last refinement, which gave the final discrepancy indices shown in Table III. The final atomic positions are given in Table IV together with their estimated standard deviations based on the final least-squares correlation matrix. Interatomic distances and angles are given in Table V.

Anisotropic thermal parameters, positional and thermal parameters of the rigid phenyl groups and the remaining hydrogen atoms, and the observed and calculated structure factor amplitudes are available as supplementary material.

Discussion of the Structure

The crystal consists of discrete molecular units of $Ru_3\{\mu\text{-}H,\mu\text{-}O{=}C(NMe_2)\}(CO)_9P(OPh)_3$ and crystallizes in the monoclinic space group *Pc* with eight molecules per unit cell. There are two independent molecules in the crystallographic asymmetric unit, referred to here as molecules A and B. Three crystal-packing diagrams viewed down the *b* axis are available as supplementary figures. Alternating parallel translational rows are seen of molecules A and B. The molecules are oriented such as to interface the phenyl groups of their triphenyl phosphite ligands on one side and the carbonyl groups of the $Ru(CO)_4$ units on the other side. Closest intermolecular approaches between oxygen atoms of carbonyl groups are those between Ru(3) or Ru(5) with Ru(6). Those below 3.10 Å are given as follows, (±0.02 Å): O(31)···O(61), 2.99; O(31)···O(63), 3.09; O(33)···O(61), 3.01; O(33)···O(64), 3.06; O(34)···O(62), 3.01; O(53)···O(64), 3.05.

Molecular Geometry: Trimetal Frame and Bridging Groups. The discussion will be based principally on molecule A; the parameters of B are similar. The molecular structure and numbering of the atoms of molecule A are depicted in Figure 3. This structure resembles closely that of the parent $Ru_3\{\mu\text{-}H,\mu\text{-}O{=}C(NMe_2)\}(CO)_{10}$ (**2**) except that a $P(OPh)_3$ ligand

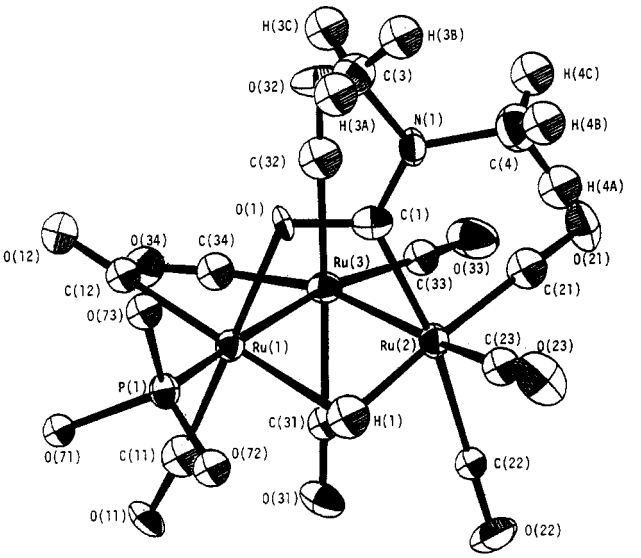

Figure 3. ORTEP projection of symmetry-independent molecule A of $Ru_3\{\mu\text{-}H,\mu\text{-}O{=}CNMe_2\}(CO)_9P(OPh)_3$. Ellipsoids represent 50% probability surfaces. Phenyl groups omitted for clarity.

is substituted for a carbonyl group trans to $Ru(CO)_4$ on the ruthenium atom bonded to the carboxamido oxygen atom. Selected interatomic distances and angles are presented in Table V. More extensive listings of interatomic distances and angles are available with the supplementary material.

Molecule A (or B) consists of a triangle of ruthenium atoms in which the bridged metal–metal separation is significantly longer than the other two (see Table V), although all three do not depart far from the mean metal separation of 2.8550 (15) Å in **2**,[5b] or of 2.8542 (4) Å in $Ru_3(CO)_{12}$.[9] There is bonding between the bridged ruthenium atoms, but we choose not to draw in the metal–metal vector.[10] The bond lengths

(9) Churchill, M. R.; Hollander, F. J.; Hutchinson, J. P. *Inorg. Chem.* **1977**, *16*, 2655–2659.

Ru(1)–H(1) and Ru(2)–H(1) (both 1.67 (18) Å) are somewhat shorter than those reported for **2** (1.73 (9) and 1.91 (9) Å)[5b] but fall well within what is expected for the bridging hydrogen.[11]

Coordination Geometry around the Metals. An approximately octahedral geometry may be recognized for the bonding of terminal or bridging groups coordinated to each of the metal atoms. Interatomic angles in Table V have been organized to illustrate this point. Comparable values with 0.5° are observed in **2** except where the phosphorus atom of the phosphite group in **5** has been substituted for the carbon of a carbonyl group in **2**. In that case, bond angles vary in the range 0.5–6.1° (see designated angles *b*–*g* in Table V and the comparison values for **2** in the footnotes of the same letters in that table).

For seven of the nine terminally bonded CO groups, the $Ru–C_{CO}$ separations fall within the range 1.910–1.975 (13) Å (see the supplementary material); this range is similar to that observed for $Ru_3(CO)_{12}$.[9] The longest $Ru–C_{CO}$ separation is associated with the carbonyl group trans to the carboxamido carbon atom, similar to what is seen in **2**.[5b] For CO groups bonded at Ru(1) (or Ru(4) in molecule B), the $Ru–C_{CO}$ separations are somewhat shorter, in the range 1.834–1.893 (13) Å. The C–O separations of these carbonyl groups fall in the range 1.10–1.16 (2) Å;[12] the Ru–C–O angles are all close to linear, ranging from 174.6 (15) to 179.8 (11)° (see the supplementary material).

Structural Features of the Carboxamido Group. Within this group the C–O and C–N separations are 1.255 (17) and 1.355 (17) Å, respectively. Comparison with standard bond lengths[12] of $C(sp^2){=}O$ = 1.20 Å and $C(sp^2)—N$ = 1.43 Å suggests delocalized bonding of the type represented by the two canonical structures I and III. The separation Ru(2)–C(1) of

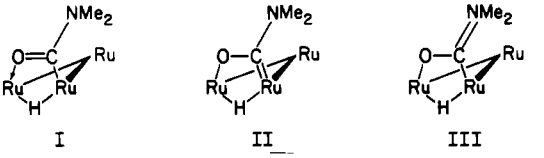

I II III

2.102 (13) Å is significantly longer than those observed for $Ru–C_{CO}$ (see above); for $C(sp^2)—Ru$ we expect 2.084 Å.[13] There is thus very little multiple-bond (carbene) character to the bridging acyl group as represented by II; this is also the case in the parent complex (**2**) or, for example, in $(OC)_3Fe\{\mu\text{-}O{=}CPh\}_2Fe)CO_3$[14] or in $(\eta^5\text{-}C_5H_5)Ir\{\mu\text{-}O{=}CMe,\mu\text{-}O{=}CPh,\mu\text{-}PPh_2\}Mn(CO)_3$.[15]

Acknowledgment. This work was supported by a grant from the National Science Foundation (Grant No. CHE-79-08406) and an SERC Fellowship to N.M.B. Major instruments used in this work were purchased with support as follows: Syntex diffractometer, NSF Grant No. GP 28248; Bruker WM-200 spectrometer, NSF Grant No. CHE-76-05926.

Registry No. **1**, 15243-33-1; **2**, 74325-95-4; [Gua][**2a**], 80845-41-6; **3**, 93425-38-8; [Gua][**3a**], 93425-40-2; **4**, 93403-56-6; [Gua][**4a**], 93403-59-9; **5**, 93403-57-7; [Gua][**5a**], 93403-61-3.

Supplementary Material Available: FTIR spectra of the carbonyl region for **2**, [Gua][**2a**], [Gua][**5a**], and **5**, listings of anisotropic thermal parameters, isotropic thermal parameters, and positional and isotropic thermal parameters for derived group atoms, full listings of interatomic distances and angles, packing diagrams, and a table of structure factors (33 pages). Ordering information is given on any current masthead page.

(10) We omit the conventional vector between metal atoms of the doubly bridged edge of the metal triangle because this representation better reflects the bonding in octahedral coordination around the metal atoms in question. Cf.: Chesky, P. T.; Hall, M. B. *Inorg. Chem.* **1983**, *22*, 3327–3335.
(11) Teller, R. G.; Bau, R. *Struct. Bonding (Berlin)* **1981**, *44*, 1–82.
(12) *Spec. Publ.—Chem. Soc.* **1965**, *No. 18*.
(13) There are few comparison structures for this type of bond, for which we may cite the following (Å): 2.169 (16) (Osella, D.; Sappa, E.; Tirripichio, A.; Camellini, M. T. *Inorg. Chim. Acta* **1980**, *42*, 183); 2.17 and 2.23 (Sappa, E.; Manotti-Lanfredi, A. M.; Tirippichio, A. *Inorg. Chim. Acta* **1980**, *42*, 255); 2.07 (4) and 2.04 (5) (Evans, M.; Hursthouse, M.; Randall, E. W.; Rosenberg, E.; Milone, L.; Valle, M. *J. Chem. Soc., Chem. Comm* **1972**, 545).
(14) (a) Fischer, E. O.; Kiener, V.; Bunbury, D. S.; Frank, E.; Lindley, P. F.; Mills, O. S. *J. Chem. Soc., Chem. Commun.* **1968**, 1378. (b) Lindley, P. F.; Mills, O. F. *J. Chem. Soc. A* **1969**, 1279.
(15) Blickensderfer, J. R.; Knobler, C. B.; Kaesz, H. D. *J. Am. Chem. Soc.* **1975**, *97*, 2686–2691.